

## Chronology for climate change: Developing age models for the Biogeochemical Ocean Flux Study cores

B. Manighetti and I.N. McCave

Department of Earth Sciences, University of Cambridge, Cambridge, England

M. Maslin

Geologisch-Palaontologisches Institut, Universität Kiel, Kiel, Germany

N. J. Shackleton

Godwin Laboratory, University of Cambridge, Cambridge, England

**Abstract.** We construct age models for a suite of cores from the northeast Atlantic Ocean by means of accelerator mass spectrometer dating of a key core, BOFS 5K, and correlation with the rest of the suite. The effects of bioturbation and foraminiferal species abundance gradients upon the age record are modeled using a simple equation. The degree of bioturbation is estimated by comparing modeled profiles with dispersal of the Vedde Ash layer in core 5K, and we find a mixing depth of roughly 8 cm for sand-sized material. Using this value, we estimate that age offsets between unbioturbated sediment and some foraminifera species after mixing may be up to 2500 years, with lesser effect on fine carbonate ( $<10\ \mu\text{m}$ ) ages. The bioturbation model illustrates problems associated with the dating of "instantaneous" events such as ash layers and the "Heinrich" peaks of ice-rafted detritus. Correlations between core 5K and the other cores from the BOFS suite are made on the basis of similarities in the downcore profiles of oxygen and carbon isotopes, magnetic susceptibility, water and carbonate content, and via marker horizons in X radiographs and ash beds.

### Introduction

Recent advances in the understanding of oceanographic changes over the last 30 ka have been possible, partly as a result of improvements in stratigraphic resolution brought about by development of accelerator mass spectrometer (AMS) radiocarbon dating. Work on a  $<30,000$  year timescale demands a very tight age control and precise correlation if robust inferences are to be made about rapid changes or events of short duration. The basic requirements are a continuous depositional record and rapid sedimentation to minimize the effects of bioturbation. This study deals with the development of an AMS-based age model for a core from the Biogeochemical Ocean Flux Study (BOFS) suite and the application of the age model to other BOFS cores by correlation.

### Location

The BOFS northern leg coring was carried out in 1989 on RRS *Discovery* cruise 184 [McCave, 1989], along a transect at approximately  $20^\circ\text{W}$ , from the lower flanks of the Mid-Atlantic Ridge at  $47^\circ\text{N}$  and the East Thulean Rise, across the South Rockall Gap, along the slopes of Rockall Bank, over

the Hatton-Rockall Basin and South Iceland Basin to Gardar Drift at  $59^\circ\text{N}$ . Fifteen kastenlot cores were recovered using a 3-m corer barrel designed by Zangger and McCave [1990], of which nine are included in this study. Their location, depth and recovered lengths are given in Table 1. Subsamples from five of the cores (5K, 8K, 11K, 14K and 17K) were analyzed for oxygen and carbon isotopes at the Godwin Laboratory, Cambridge, and based upon these results, core 5K was selected for AMS dating. Each core was subsectioned, X rayed, probed for bulk magnetic susceptibility and sampled to determine water content. Wet sieving yielded the proportions greater and less than  $63\ \mu\text{m}$ , and magnetic susceptibility was then measured on the coarse and fine fractions. Total- and carbonate-carbon analysis was carried out on the whole sediment and the fine fraction (see also Manighetti and McCave, this issue).

### Methods

AMS  $^{14}\text{C}$  dating was carried out on monospecific samples of the planktonic foraminifera *Globigerina bulloides*, *Neoglobigerina pachyderma* (s) and *Globorotalia inflata* by M. Arnold and J-C Duplessy at Gif-sur-Yvette. *G. bulloides* and *G. inflata* samples were picked from the 300-355  $\mu\text{m}$  fraction and *N. pachyderma* (s) from the the 250-300  $\mu\text{m}$  fraction. Oxygen and carbon stable isotopic measurements were made at Cambridge on VG Sira Series II and Prism mass

Copyright 1995 by the American Geophysical Union.

Paper number 94PA03062  
0883-8305/95/94PA-03062\$10.00

**Table 1.** Details of Core Locations

Discovery Station	Core	Latitude	Longitude	Water Depth, m
11882/4	5K	50°40.9'N	21°52.0'W	3547
11883/3	6K	51°07.0'N	21°11.9'W	2865
11884/4	7K	51°45.3'N	22°32.5'W	2327
11886/2	8K	52°30.1'N	22°04.2'W	4045
11889/2	9K	53°41.6'N	21°19.5'W	3268
11890/2	10K	54°39.9'N	20°39.0'W	2777
11891/4	11K	55°11.5'N	20°21.1'W	2004
11896/1	14K	58°37.2'N	19°26.2'W	1756
11905/1	17K	58°00.2'N	16°29.8'W	1150

spectrometers [see *Shackleton and Hall*, 1989]. Bulk magnetic susceptibility was measured with a Bartington Instruments MS2 meter and a probe-type sensor held against sediment slabs. Coarse and fine fraction magnetic susceptibility was also measured on dried samples using a Bartington MS2B sensor with a 36-mm internal diameter. Total, carbonate and organic carbon contents were determined using a Carlo Erba 1106 elemental analyzer, according to the method of *Manighetti* [1993], and grain size distributions were investigated by wet sieving at 63  $\mu\text{m}$  followed by analysis on a SediGraph 5000ET with a computer interface devised by *Jones et al.* [1988].

## Developing an Age Model for Core 5K

### AMS Dating

The age model for the northern BOFS core suite is based upon AMS dating of core 5K from the East Thulean Rise. In addition to good resolution of features in its oxygen isotopic profiles, core 5K possesses distinct correlatable horizons such as the Vedde Ash and deposits of the latest four ice-rafting pulses known as "Heinrich events" [*Heinrich*, 1988; *Broecker et al.*, 1992]. The AMS dates on BOFS 5K are shown in Table 2, and plotted against depth downcore in Figure 1.

The  $^{14}\text{C}$  dates in Table 2 were calculated using the Libby half life of 5568 years, and converted to "calendar ages" using the marine calibration datasets of *Stuiver and Braziunas* [1993] and *Bard et al.* [1993a] with the program Calib-3.0 [*Stuiver and Reimer*, 1993]. The *Stuiver and Braziunas* [1993] dataset incorporates a time-dependent world ocean reservoir correction averaging 409 years, back to 11,400 cal B.P. The *Bard et al.* [1993a] calibration of ages between 11,400 and 21,950 cal B.P. is based on coral samples which record the local regional (and variable) reservoir deficiency of unknown magnitude (but often estimated at a constant 400 years). Beyond 21,950 years B.P., there is insufficient evidence for a detailed calibration of  $^{14}\text{C}$  to calendar years, but sparse coral data indicate that the offset is at least as large at 30 ka as at 20 ka (Paula Reimer, personal communication, 1993). Older  $^{14}\text{C}$  dates have therefore been "calibrated" by applying a constant offset, of +3182 years, representing both the difference due to  $^{14}\text{C}$  activity changes, the reservoir correction

**Table 2.** Accelerator Mass Spectrometer Dates for Core 5K

Depth, cm	Foram Species	Marine $^{14}\text{C}$ Age	1 $\sigma$ Error	Estimated Atmospheric $^{14}\text{C}$ Age	Calibrated Age
0	<i>G. bulloides</i>	2,020	140	1,620	1,556
20	<i>G. inflata</i>	4,970	130	4,570	5,292 <sup>a</sup>
38	<i>G. bulloides</i>	8,860	130	8,460	9,462 <sup>a</sup>
44	<i>G. inflata</i>	14,970	180	14,570	17,447
46	<i>G. bulloides</i>	11,180	150	10,780	12,709 <sup>b</sup>
46	<i>N. pachyderma</i> (s)	10,770	130	10,370	12,257 <sup>b</sup>
73	<i>G. bulloides</i>	12,860	150	12,460	14,590
74	<i>G. bulloides</i>	12,990	160	12,590	14,781
74	<i>N. pachyderma</i> (s)	15,370	180	14,970	17,884 <sup>a</sup>
78	<i>N. pachyderma</i> (s)	16,520	180	16,120	18,995
80	<i>N. pachyderma</i> (s)	16,510	170	16,110	18,985 <sup>a</sup>
90	<i>N. pachyderma</i> (s)	17,650	220	17,250	20,472 <sup>a</sup>
100	<i>N. pachyderma</i> (s)	20,210	280	19,810	23,392 <sup>a</sup>
114	<i>N. pachyderma</i> (s)	22,960	330	22,560	26,142 <sup>a</sup>
130	<i>N. pachyderma</i> (s)	25,300	400	24,900	28,482 <sup>a</sup>
148	<i>N. pachyderma</i> (s)	28,800	530	28,400	31,982 <sup>a</sup>
202	<i>G. bulloides</i>	35,500	1100	34,800	38,682 <sup>c</sup>
202	<i>N. pachyderma</i> (s)	35,200	1000	35,100	38,382 <sup>c</sup>
238	<i>N. pachyderma</i> (s)	30,440	630	30,040	33,622

<sup>a</sup> Date used in age model

<sup>b</sup> Average of these dates used as 46 cm age

<sup>c</sup> Average of these dates is used as 202 cm age

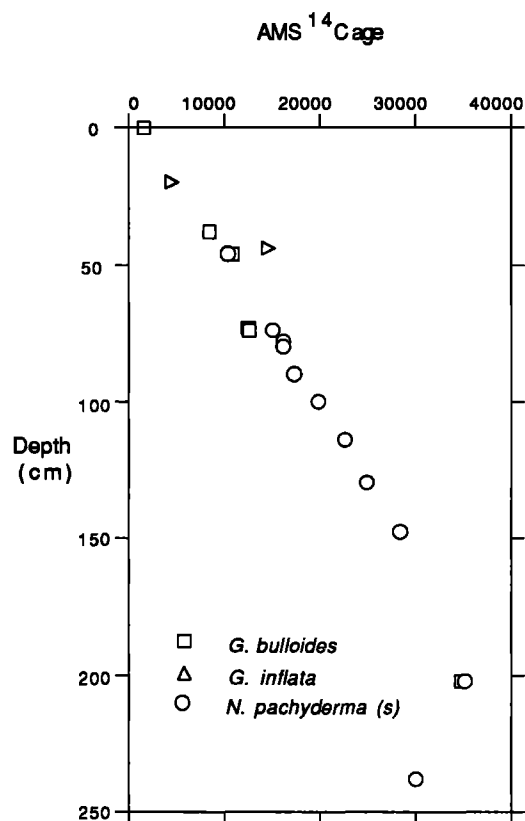


**Figure 1.** AMS <sup>14</sup>C ages against depth in core 5K. Dates determined on *G. bulloides* samples are shown as squares, while *N. pachyderma* (s) dates are shown as circles and *G. inflata* as triangles.

for marine samples, and a correction taking account of the use of the Libby half life rather than the true value of 5730 years.

It is not feasible to use every date in Table 2 to create the age model, since age inversions occur and dates determined on different species at the same depth interval may differ widely. As suggested by Broecker *et al.* [1984] and demonstrated by Andree *et al.* [1984], Peng and Broecker [1984] and Bard *et al.* [1987], in the presence of species-abundance gradients, age biases may be generated, particularly where accumulation rates are low. By considering what is known of planktonic foraminiferal species abundance in the area through time, and the mechanism of bioturbation, it is possible to determine which dates are the most reliable.

### Species Abundance and Bioturbation

It has been widely documented that the abundance of the species *N. pachyderma* (s) changes between glacial and interglacial times in Atlantic sediments of middle latitudes [e.g. Ruddiman and McIntyre, 1976; Ruddiman *et al.*, 1977; Bard *et al.*, 1987; Broecker *et al.*, 1988a]. It is the single planktonic foraminifera with a preference for polar waters [Kipp, 1976], and therefore an indicator of low temperatures in surface waters. In parts of the North Atlantic, it reached almost 100% of the total planktonic foraminifera count (>150  $\mu$ m) during glacial times [Ruddiman and McIntyre,

1981; Maslin, 1993]. In warmer periods, however, it is largely replaced by an assemblage of subpolar and transitional species, including *G. bulloides* and *G. inflata*. The abundance of *N. pachyderma* (s) and *G. bulloides* with depth in core 5K is shown in Figure 2.

If the abundance of a species used for radiocarbon dating changes with depth downcore, then bioturbation will introduce age biases in the portion of the record where the gradient occurs. An example of such a gradient occurs in the records of the species *N. pachyderma* (s) and *G. bulloides* across Termination 1 (Figure 2), and may explain the large discrepancy (3100 calendar years) between the ages measured on these two species at 74 cm (Figure 2). The glacial abundance of *G. bulloides* is usually under 1%, while *N. pachyderma* (s) is as high as 16%, as a weight percentage of total sediment. In the Holocene, the abundance of *G. bulloides* rises to ~2-4%, while *N. pachyderma* falls to below 1%. Mixing of sediment across the Termination will introduce relatively abundant, younger *G. bulloides* to older, *bulloides*-poor levels further down. By contrast, fewer young *N. pachyderma* will be mixed down from above the termination, where they are scarce, so that the *N. pachyderma* (s) date is likely to be more reliable.

For the purpose of flux calculations, the age model must give a zero age for the sediment surface, rather than an average age of the mixed layer (dated 1556 calendar years on a *G. bulloides* sample from the uppermost centimetre of the core). However, it may be incorrect to assign a zero age to the core top, since during recovery of kastenlot cores, a small amount of material is usually lost. The core top age is therefore estimated by extrapolating the sedimentation rate between two Holocene dated points (20 and 38 cm) upward to give a surface intercept of 659 calendar years. At a sedimentation rate of 4.32 cm ka<sup>-1</sup>, this implies a loss from the core top of 2.85 cm, which seems a reasonable estimate of the recovery of surfaces in kasten coring. Assuming homogeneity, the present mixed layer can be estimated at about 7 cm.

The *G. inflata* date at 44 cm (17447 calendar years) is anomalous, significantly higher than dates immediately below, and apparently about 5 ka too old. The very large amount of older material required to produce such a discrepancy probably precludes contamination as the cause of the error. It is also unlikely that the sample interval was wrongly identified, since the abundance of *G. inflata* remains below picking levels through the glacial until around 64 cm, corresponding to roughly 15.5 ka based on other AMS dates in the core. At 17.5 ka there are hardly any *G. inflata* present. For this reason too, bioturbation could not account for the result, and we cannot satisfactorily explain the anomaly. At 46 cm, the dates on *G. bulloides* and *N. pachyderma* (s) coincide within 2 $\sigma$  errors (Table 2), both species are at similar levels of abundance (Figure 2), although *N. pachyderma* is on the decline, and might be expected to generate an older date than *G. bulloides*, whose abundance is roughly constant. An average of the two dates is used for the 46 cm horizon in the 5K age model.

At 78 and 80 cm, two *N. pachyderma* (s) dates fall within 10 years of each other, and the date at 80 cm is included in the model since it lies more directly on the age-depth trend in

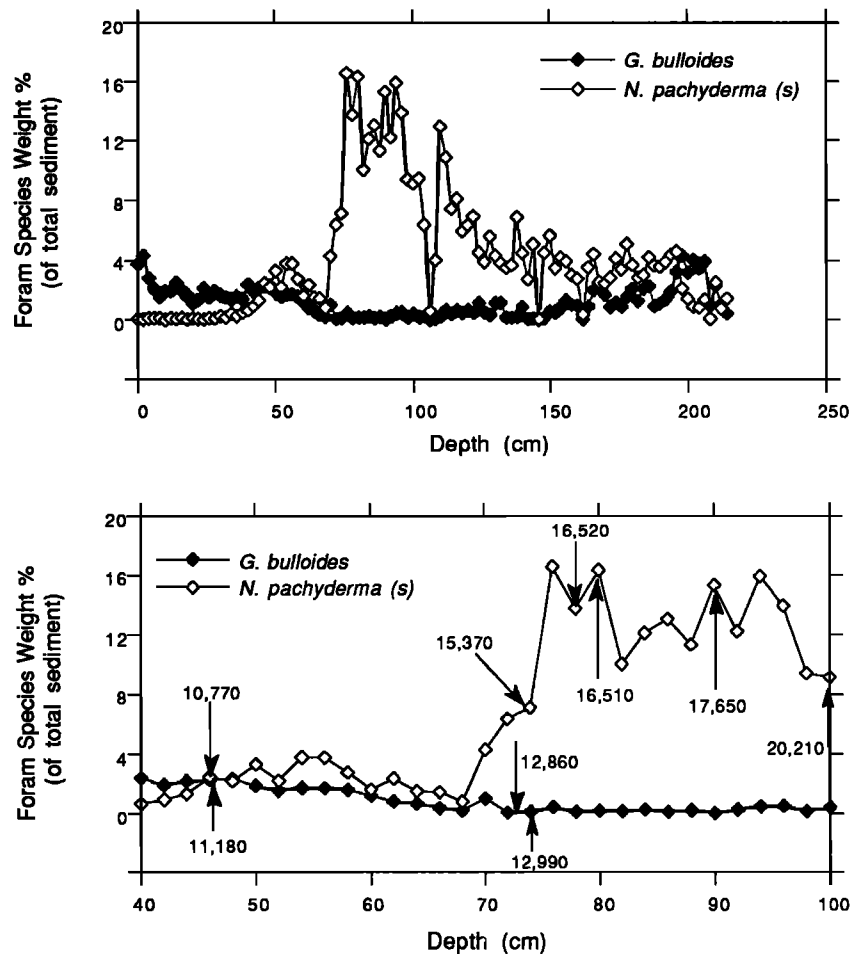


**Figure 2.** Abundance of the foram species *G. bulloides* and *N. pachyderma* (s) with depth in core 5K, expressed as a weight percentage of the total sediment. Detail of the interval 40-100 cm shows the location of AMS  $^{14}\text{C}$  dated samples on the abundance curves, and the large offset between *G. bulloides* and *N. pachyderma* (s) ages at 74 cm.

Figure 1. The *N. pachyderma* (s) age at 238 cm lies well off the main trend in Figure 1, and is reversed with respect to *G. bulloides* and *N. pachyderma* ages from 202 cm. This is presumably a result of contamination with younger material, which causes relatively greater errors as sample age increases. This date, and that of the *G. inflata* sample at 44 cm, are not included in the age model.

The age model was constructed by linear interpolation between the chosen eleven calibrated AMS dates and inferred core top age, and extended below 202 cm by using the average sedimentation rate in the core ( $5.33 \text{ cm ka}^{-1}$  calendar years, 0-202 cm). The model is illustrated in Figure 3 showing calibrated age versus depth, and giving the sedimentation rates over different segments of the record. This model minimises the impact of bioturbation of steep abundance gradients on age estimates. Nevertheless, these gradients are present, both in the foraminiferal abundances and several other properties. We therefore wish to assess the likely magnitude of age offsets due to bioturbation, and in the next section examine this problem using a simple homogenous mixing model.

### Bioturbation: A Simple Model

In the simplest type of bioturbation model, mixing takes place within the sediment to a given depth, and is assumed to completely homogenize the "bioturbation box" within a timescale short relative to the sedimentation rate [Berger and Heath, 1968]. The mechanism of bioturbation is as described by Bard *et al.* [1987] in their attempt to deconvolve isotopic records for the last deglaciation, and contains no diffusion gradient. The following development reaches the same conclusion as Bard *et al.* [1987] in a simple arithmetical manner.

Consider a sediment column which is homogeneously mixed to a depth  $H$ , with a concentration of a particular foram species  $C_0^{\text{orig}}$ . Sediment is added to the column in increments corresponding to the thickness of the sampling interval  $x$ . The new sediment has a concentration of the foraminiferal species,  $C_1^{\text{orig}}$ . This is then mixed thoroughly with underlying material to a depth of  $H$ , producing a homogenous layer with a concentration of the foram species  $C_1^{\text{new}}$ . A homogenous layer of  $C_0^{\text{orig}}$ ,  $x$  thick, remains below the new mixed layer.

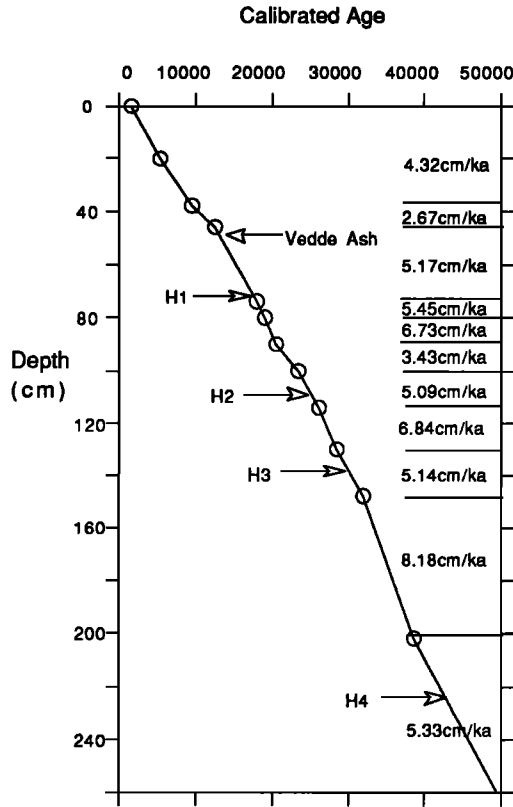


Figure 3. Calibrated age model for core 5K, based upon AMS <sup>14</sup>C dates selected as described in text. The position of the Vedde Ash and Heinrich events 1-4 are marked.

New increments are continually added to the column, building up a pile of homogeneously mixed layers. This may be expressed as follows:

The measured (bioturbated) value of foraminiferal abundance in increment *y* is given by

$$C^n_y = \left(\frac{x}{H}\right)C^o_{y+[(H/x)-1]} + \left(1 - \frac{x}{H}\right)C^n_{y-1} \quad [1]$$

and the "original" value of foraminiferal abundance in the same interval is

$$C^o_y = \frac{C^n_{y-[(H/x)-1]}}{(x/H)} - \frac{\left(1 - \frac{x}{H}\right)C^n_{y-(H/x)}}{(x/H)} \quad [2]$$

which may be rearranged to

$$C^o_y = (H/x)C^n_{y-(H/x)+1} + [1-(H/x)]C^n_{y-(H/x)} \quad [3]$$

As shown by Bard et al. [1987], an AMS age record or isotopic signal can be deconvolved simply by working with the product: (carrier concentration times age) or (carrier concentration times isotopic ratio)

Because of the small number and wide spacing of the AMS dates, deconvolution cannot be carried out on the measured AMS-dated intervals alone. However, it would be misleading to attempt a deconvolution of linearly interpolated age models

based on *G. bulloides* and *N. pachyderma* (s) dates, since it is highly unlikely that following bioturbation in the presence of species abundance gradients, ages would maintain linearity. What is more revealing is to assess whether a linear age sequence can be theoretically "bioturbated" to produce offsets of over 3000 years, given the observed species abundance changes downcore, and by employing a realistic mixing depth. To determine the characteristic mixing depth for sand-sized material in BOFS 5K, we examined the dispersal of coarse fraction sediment from an instantaneously deposited layer, the Vedde Ash [Mangerud et al., 1984].

In Figure 4a, the number of sand-sized rhyolitic shards per gram of total sediment is plotted against depth downcore. The bioturbated ash profile in core 5K is asymmetrical, with a fairly sharp base and gradational top. This resembles the curve generated by simple model bioturbation, although the base is more diffuse than the model predicts. By plotting the natural log of ash abundance against depth, the observed curve may be compared with theoretical homogenous bioturbation of an ash layer with different values of *H* (the bioturbation depth) and a sampling interval *x* = 2cm (Figures 4b and 4c). As *H* increases, the gradient of the log abundance line decreases in the model, in a manner which enables the characteristic value of *H* to be estimated for the 5K ash profile. In 5K, the best fit line through the log data has a gradient of 0.162 and corresponds most closely to theoretical bioturbation using a mixing depth *H*=8 cm. This is typical for deep marine environments [Nozaki et al., 1977; Peng et al., 1977] and similar to the mixing depth determined for the Holocene by bulk <sup>14</sup>C and <sup>210</sup>Pb<sub>excess</sub> profiles on BOFS box core samples [Thomson et al., 1993a, b], suggesting that the assumption of homogenous bioturbation to a constant depth below the surface is a reasonable first approximation.

This study also illustrates the problem associated with the use of "instantaneous" marker horizons for age modeling purposes. With a mixing depth of 8 cm, an ash layer deposited at *n* centimetres in a core will appear at peak abundance *n-H* cm (8 cm) below its original position, following bioturbation (Figure 4d). The age of the ash layer measured on land (in deposits not subject to bioturbation) is therefore unlikely to correspond to the age of foraminifera mixed in with the ash in marine deposits, since the abundance of foraminifera used for dating does not vary as markedly as the ash grains. The problem is much more acute, of course, in cores with a low sedimentation rate: at an average of 2 cm ka<sup>-1</sup>, an 8 cm displacement makes a difference of 4000 years, whereas at 20 cm ka<sup>-1</sup>, the difference is only 400 years.

To investigate the possible effects of homogenous bioturbation to a depth of 8 cm on the ages recorded by *N. pachyderma* (s) and *G. bulloides*, it is first necessary to "deconvolve" the species abundances, using equation 3 (Figure 5). A simple, linear age sequence is then 'bioturbated' with each of the restored species abundance profiles. This yields two separate age models, one for each species, which can then be compared with the "true age" at any depth. The method was attempted using 5K species abundance data and a linear age model from zero to 28,482 years, the (calibrated) age recorded by a *N. pachyderma* (s) sample at 130 cm depth. For modelling purposes, this age was assumed to have remained unchanged following bioturbation. In certain cases

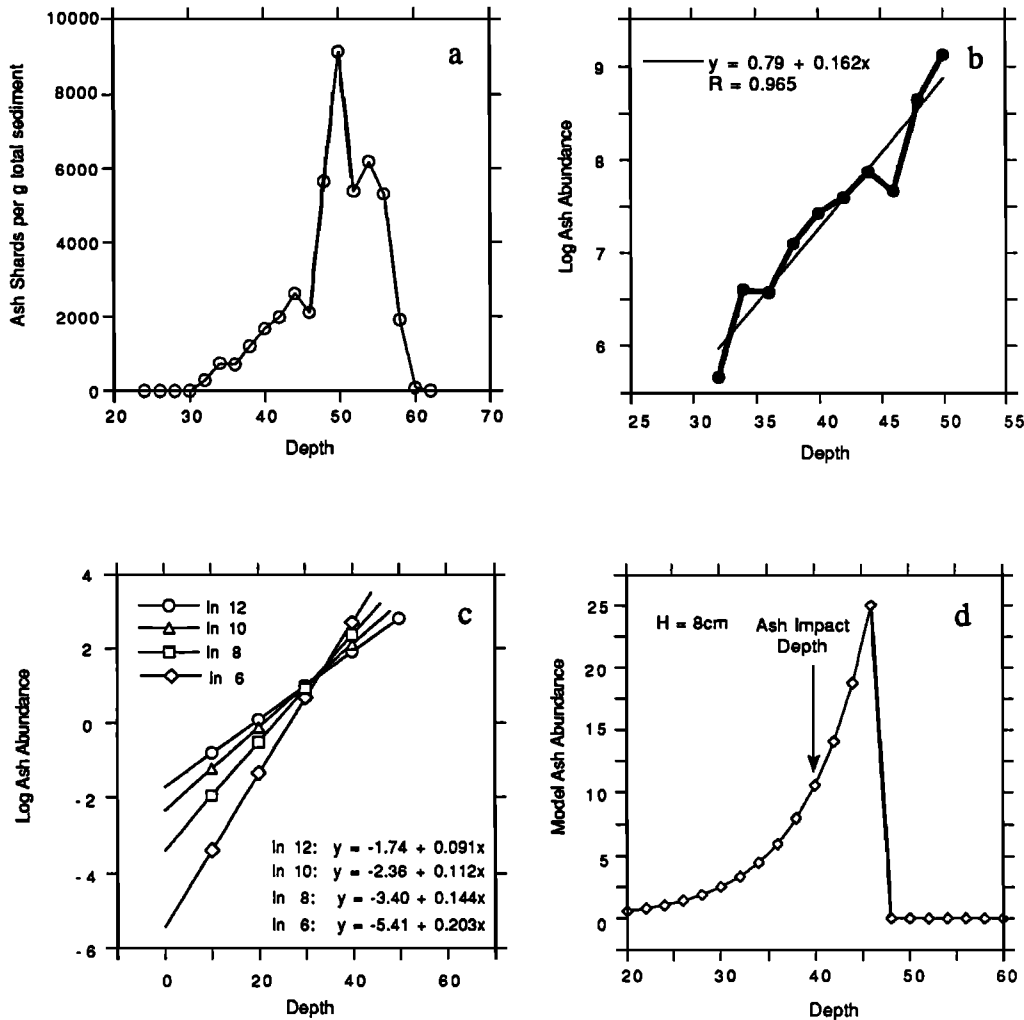


**Figure 4.** (a) Number of clear (rhyolitic) ash shards  $>63 \mu\text{m}$  per gram of total sediment with depth in core 5K. (b) Natural logarithm of the ash abundance with depth in core 5K. (c) Natural log of theoretical abundance profiles following bioturbation with different values of  $H$ . The profile for  $H = 8 \text{ cm}$  most closely resembles the observed log abundance curve in Figure 4b. (d) Model bioturbation of an ash layer with  $H = 8 \text{ cm}$ , displacing the ash peak downward from the original impact depth.

of very low measured abundance, the deconvolution actually yielded negative species abundance values. To facilitate the modeling these were altered to 0.01%.

The offset between the original (or "true") age and each of the "bioturbated" models is illustrated in Figure 6. This shows that ages recorded by *N. pachyderma* (s) in Holocene sediment (0-50 cm) would be far greater than the true age, due to the very low abundance of this species following the termination. It is most unlikely, though, that dating would ever be carried out on *N. pachyderma* (s) over this time interval, when there are many other species of greater abundance available. Across the transition from glacial to Holocene, however, species abundances are more variable, and the ages measured on *N. pachyderma* (s) and *G. bulloides* depart quite markedly from each other around 55-75 cm, close to the termination as recorded in oxygen isotopes. The difference between them is up to 2500 years, with *N. pachyderma* (s) older than *G. bulloides*, which is similar to the offset observed in AMS

dates for core 5K at 74 cm. The maximum age offset observed in the model occurs at slightly shallower depths than in the 5K AMS data (66 cm compared to 74 cm), but this may be partly due to the simplicity of the assumed original age model. In reality, sedimentation rates probably varied from glacial to Holocene times.

The abundance of components other than foraminifera also changed from glacial to Holocene times, and the ages recorded by these components may be offset from those of foraminifera or other constituents with which they are mixed. In particular, the fine carbonate ( $<10 \mu\text{m}$ ) associated with coccoliths varies from around 80 to less than 40% by weight of the total sediment in core 5K. The effect of this upon ages that might be measured on the fine carbonate fraction is shown in Figure 6. The model assumes that bioturbation of the fines occurs in the same manner and to the same extent as for the sand fraction. Maximum offset is observed, as expected, at the transition from glacial to Holocene, occurring between 60 and

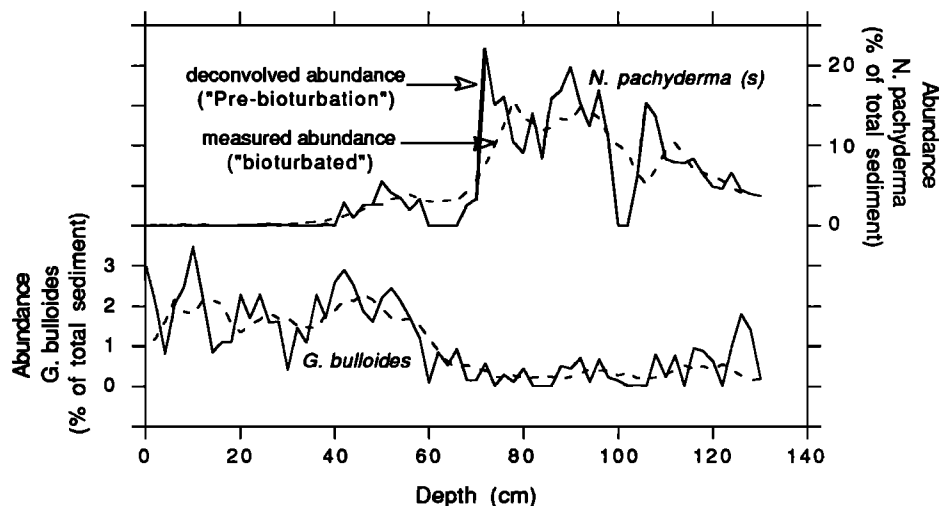


**Figure 5.** Measured and deconvolved abundances of the foram species *G. bulloides* and *N. pachyderma* (s). Abundances are expressed as weight percentage of the total sediment. The deconvolution was made using a bioturbation depth  $H$  of 8 cm and a sampling interval of 2 cm.

80 cm, but is only about 300 years greater than the true age.

Vertical biodiffusivity may be size-dependent, such that larger particles are less deeply mixed, and evidence suggests that the diffusivity of 250  $\mu\text{m}$  sand is about a factor of 10 less than 10  $\mu\text{m}$  silt [Wheatcroft, 1992]. In the simple bioturbation model used in this work, diffusion is regarded as operating infinitely fast with respect to the sedimentation rate. All size fractions would therefore record similar ages, provided no abundance gradients exist between them, even if the value of  $H$  varied with size. In reality, though, rates of deposition may be fast enough to preserve diffusional gradients [e.g. Guinasso and Schink, 1975, Schiffelbein, 1985]. This means that for the same sedimentation rate, different size fractions may be mixed to different depths (finer,

deeper), causing age offsets between them, apparently independent of abundance gradients. Age discrepancies between size fractions have been documented by Paull *et al.* [1991] in cores from the subtropical Atlantic, and have also been noted in BOFS box cores (J. Thomson *et al.*, submitted manuscript, 1995), although Ruddiman *et al.* [1980] found no evidence for a size-dependence for bioturbation of size fractions between 10 and 250  $\mu\text{m}$ .

### Correlation Between Cores

Following completion of the AMS-based age model for core 5K, the final stage is to make correlations between 5K and the other cores from the suite, assigning  $^{14}\text{C}$  and

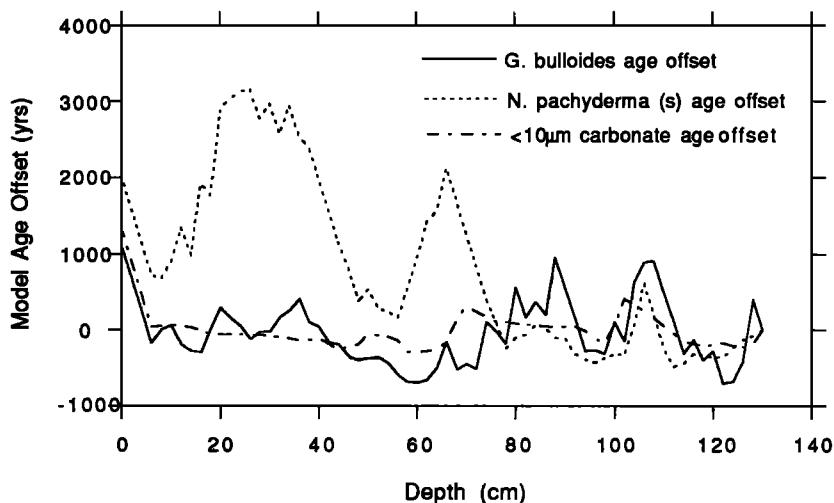


**Figure 6.** Offset between the model (linear) age and bioturbated ages recorded by *G. bulloides*, *N. pachyderma* (s) and fine (<10  $\mu\text{m}$ ) carbonate, based upon measured abundance profiles. The maximum offsets occur in the transition from glacial to Holocene, around 60-80 cm depth, where gradients in abundance are most pronounced.

"calendar" ages, and interpolating between the dated points. Correlation is effected on the basis of "landmarks" in downcore properties. Because the material is bioturbated, a landmark in one property (e.g.  $\delta^{18}\text{O}$  on sand-sized foraminifera) may not correspond in age to that of another (e.g. silt and clay fraction  $\text{CaCO}_3$  content). Additionally, "lithological", "biological" or "chemical" equivalence does not necessarily guarantee chronological correlation. AMS dating of core 5K was carried out on the large forams (250-350  $\mu\text{m}$ ), and the age model is therefore most directly applicable to the medium sand fraction (250-500  $\mu\text{m}$ ).

### Oxygen and Carbon Isotopes

Oxygen and carbon isotopic measurements were made on two species of planktonic foraminifera, *G. bulloides* and *N. pachyderma* (s), from five of the BOFS cores, 5K, 8K, 11K, 14K and 17K. The most readily identifiable event in the profiles is the transition in  $\delta^{18}\text{O}$  from heavy to light values corresponding to Termination 1A. As a result of gradients in species abundance, discussed earlier, the precise position of this event differs between species, with the *G. bulloides* termination occurring at a deeper level, making it important to compare the same species. The base of Termination 1A as defined in *G. bulloides* of core *x* will not be time equivalent to the base defined in *N. pachyderma* (s) from core *y*. Correlation of the  $\delta^{18}\text{O}$  *G. bulloides* profiles is shown in Figure 7, and details are given in Table 3. The core top value of  $\delta^{18}\text{O}$  varies

between sites in a systematic way, reflecting a north-south temperature gradient across the area (from 12.2°C at site 14K to 16.8°C south of site 5K [Lunel, 1990]). In core 14K, the sedimentation rate is sufficiently slow (average 1.64  $\text{cm ka}^{-1}$ ) and the core sufficiently long (224 cm) that the stratigraphy extends back to the stage 5e/6 boundary or Termination 2. This event is assigned an age of 128,000 years [Imbrie et al., 1984].

In the case of carbon, the surface water  $^{13}\text{C}/^{12}\text{C}$  ratio incorporated into the planktonic foram test will depend upon the degree to which organic production has depleted the  $^{12}\text{C}$ . This may be affected by the position of the polar front and could lead to downcore variations that are not synchronous across the area. The incorporation of metabolic  $\text{CO}_2$  into the test by some species can also lead to disequilibrium with respect to seawater  $\Sigma\text{CO}_2$  [Erez, 1978]. In general, oxygen isotopes are preferred over carbon isotopes for correlation purposes, but  $\delta^{13}\text{C}$  may provide support for correlations established in other measured properties.

### X-Radiography

The BOFS cores benefit from X radiographs taken on board ship which reveal internal structure, and provide a good means of identifying turbidites, repenetration of the core barrel or evidence of discontinuous or disturbed sedimentation. A number of horizons appear to be directly correlatable between cores, showing up as dark, X ray opaque bands, commonly

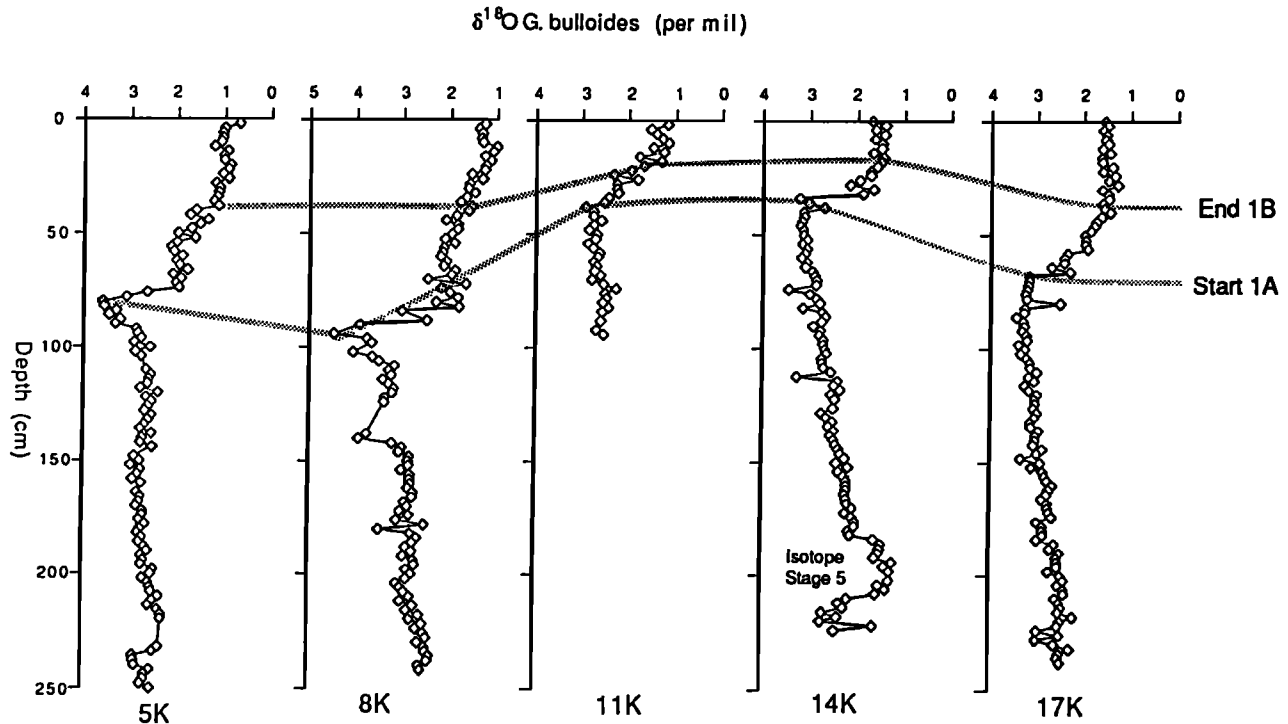


Figure 7.  $\delta^{18}\text{O}$  with depth measured on *G. bulloides* in cores 5K, 8K, 11K, 14K and 17K, showing the correlation at the start of Termination 1A. The core top values vary systematically with latitude, reflecting the fall in surface water temperature northward across the BOFS area.



**Table 3.** Depths of Landmarks in Various Properties Used for Correlation in BOFS Cores 5-11K, 14K and 17K

Core	Property	End 1B <i>G. bulloides</i>	Vedde Ash	H1	Start 1A <i>G. bulloides</i>	H2	H3	H4	H5	H6	5d/e <i>G. bulloides</i>	5e/6 <i>G. bulloides</i>	H7
<b>Event Age</b>													
Calendar Years													
	<sup>14</sup> C years <sup>a</sup>	9,462	12,152	17,497	18,985	25,159	31,204	43,088	54,700	69,700	107 ka	128 ka	130 ka
		8,460	10,300	14,654	16,110	21,578	27,622	39,129	54,700	69,700	107 ka	128 ka	130 ka
5K	$\delta^{18}\text{O}$ <i>G. bulloides</i>	38			80								
5K	MS		50	72		109	144	226					
5K	X ray			72		109		226					
6K	MS		22	34		60		132	174	216			
6K	X ray			34		60		136	175	212			
7K	MS			32		42		82	102	124			
7K	X ray					42		83	103	125			
8K	$\delta^{18}\text{O}$ <i>G. bulloides</i>	40			92								
8K	MS		54	76			180/172	242/234					
8K	X ray			76		134/126		242/234	(turbidite 124-132 cm)				
9K	MS		36	50		82		142	178				
9K	X ray												
10K	MS		66	96		176/163	226/212		(turbidite 120-133 and 165-166 cm)				
11K	$\delta^{18}\text{O}$ <i>G. bulloides</i>	18			38								
11K	MS		26			48	60						
11K	X ray					48							
14K	$\delta^{18}\text{O}$ <i>G. bulloides</i>	18									184	208	
14K	MS				34	54	76	108	122	140			212
14K	X ray					54				141			213
17K	$\delta^{18}\text{O}$ <i>G. bulloides</i>	40			68								
17K	MS			62		90	112	150	188	230			
17K	X ray							150	188				

<sup>a</sup> Carbon 14 years are calculated using the Libby half life (see text) and are corrected for the age of surface waters by -400 years. All depths in centimeters. Where two depths are given (8K and 10K), these refer to original depth and depth excluding turbidite intervals. The age for each event is derived from the 5K calibrated AMS <sup>14</sup>C age model.

with sharp bases and gradational tops. In the core descriptions, it is clear that they correspond to gravel-rich layers, sometimes several centimetres thick, which represent peaks of ice-rafted detritus ("Heinrich layers" [Heinrich, 1988; Broecker *et al.*, 1992]).

### Dating of Heinrich Events

The Heinrich layers are visible in X radiographs because of the high proportion of relatively dense lithic fragments, decreasing the water content and rendering the sediment opaque to X rays. Deposition of this material probably took place during basin-wide "events" which were essentially synchronous throughout the BOFS area. The layers are therefore considered a reliable basis for true time correlation. The quantity and coarseness of the ice-rafted detritus make it unlikely that their positions could be substantially altered by bioturbation, although upward dispersal and secondary layers may occur as noted by McCave [1988]. The layers thus present an interesting temporary "block" in the bioturbation process with the hemipelagic sediment immediately above a layer containing little or no older material from below it. This preserves a fossil mixed layer below each Heinrich zone, and means that an attempt to date the event by sampling forams immediately below it may give misleading results. Even without the presence of species abundance gradients, the foraminiferal age immediately below would be too old by the age of the mixed layer (Figure 8). However, the dramatic drop in foraminiferal abundance which took place during the ice-

rafting events is also likely to cause a bias in the age record from forams above the Heinrich layers. These would tend to be younger than the bulk sediment age for some distance above each event.

By interpolation between AMS dates in core 5K, the ages assigned to the first four Heinrich events are 17,500, 25,150, 31,200 and 43,100 calendar years, (corresponding to atmospheric  $^{14}\text{C}$  ages of 14,654, 21,578, 27,622 and 39,129 years, respectively). The earlier Heinrich events, 5, 6 and 7 (peak 11 of Heinrich, [1988]) are outside the scope of the 5K AMS age model, but have been dated by other workers via extrapolation of  $^{14}\text{C}$ -AMS-based sedimentation rates [Bond *et al.* 1992; 1993] and by interpolation between oxygen isotope events [Heinrich, 1988; Broecker *et al.*, 1992; Grousset *et al.*, 1993]. If the atmospheric  $^{14}\text{C}$  age for Heinrich peak 4, determined from the 5K AMS model, is incorporated into the model for core 14K, interpolation between it and the stage 5e/6 boundary yields ages for peaks H5 and H6 of 51,300 and 67,000 years. These closely resemble the values obtained by Bond *et al.* [1992], (52,000 and 69,000) and Broecker *et al.* [1992] (50,000 and 60,000-70,000). However, if the "calibrated" age of H4 is used instead, the ages for peaks H5 and H6 become 54,700 and 69,700. The age of the oldest Heinrich layer recovered in core 14K is estimated at 130,000, because of its position immediately below the stage 5e/6 boundary. These ages are used to construct portions of age models extending beyond the range of core 5K. In Table 3 the correlations between cores based upon the position of ice-rafting peaks visible in the X radiographs are given.

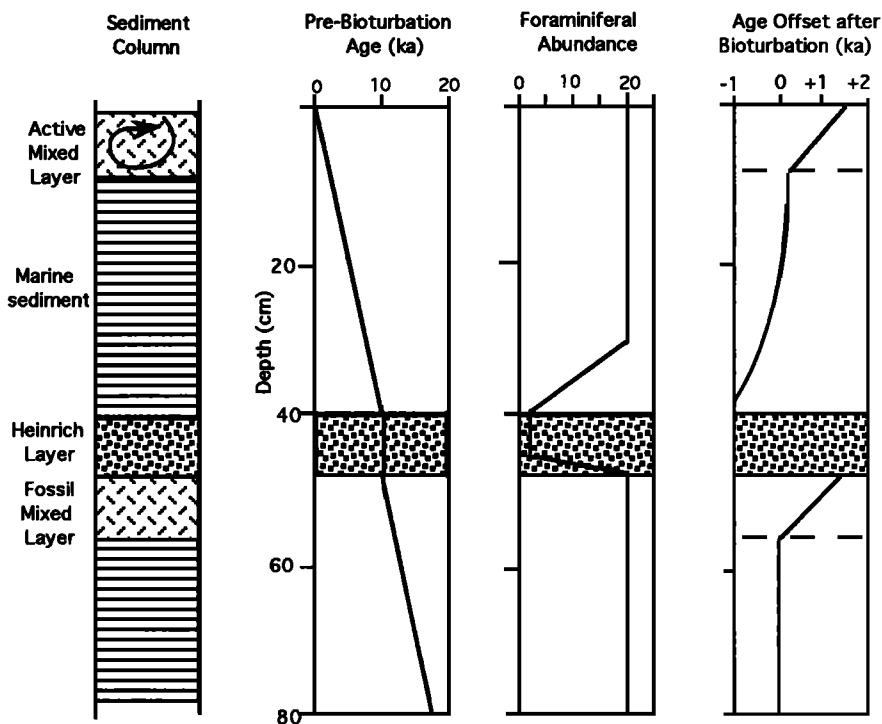


**Figure 8.** Simple model demonstrating the age offsets which may occur above and below Heinrich layers, as a result of blocking the bioturbation process. A fossil mixed layer is preserved beneath the ice-rafted detritus, in which ages of foraminifera tend to be older than pre-bioturbation values. Above the Heinrich zone, foraminiferal ages will be younger than pre-bioturbation values, as a result of homogenization of a new mixed layer.

**Magnetic Susceptibility and Water Content**

Measurements of bulk magnetic susceptibility (BMS) were made on fresh sediment slabs following X radiography (Figure 9) and on coarse and fine fractions after drying. The most prominent features of the BMS profiles correspond to the ice-rafting pulses, which delivered a quantity of lithic material of diverse mineralogy to the sea bed. In some cases, peaks of ice rafting may be identified in BMS which do not show up on the X radiographs. In Figure 9, the more southerly cores, 5, 6 and 7K, show the most marked expression of the ice-rafting

pulses. Some of these events are more obvious than others in BMS with peak "H3" (Heinrich layer 3) being absent in many profiles. In addition to these events, a minor increase in BMS is often observed at the depth of the Vedde Ash, and provides a guide to recognition of the ash in the coarse fraction microscopically.

Where doubt exists over the exact location of a peak, water content measurements can sometimes help to refine the choice of position. At 4-cm intervals, however, the measurements are too widely spaced to be of much value for correlation in cores with low sedimentation rates. The Heinrich layers as seen in

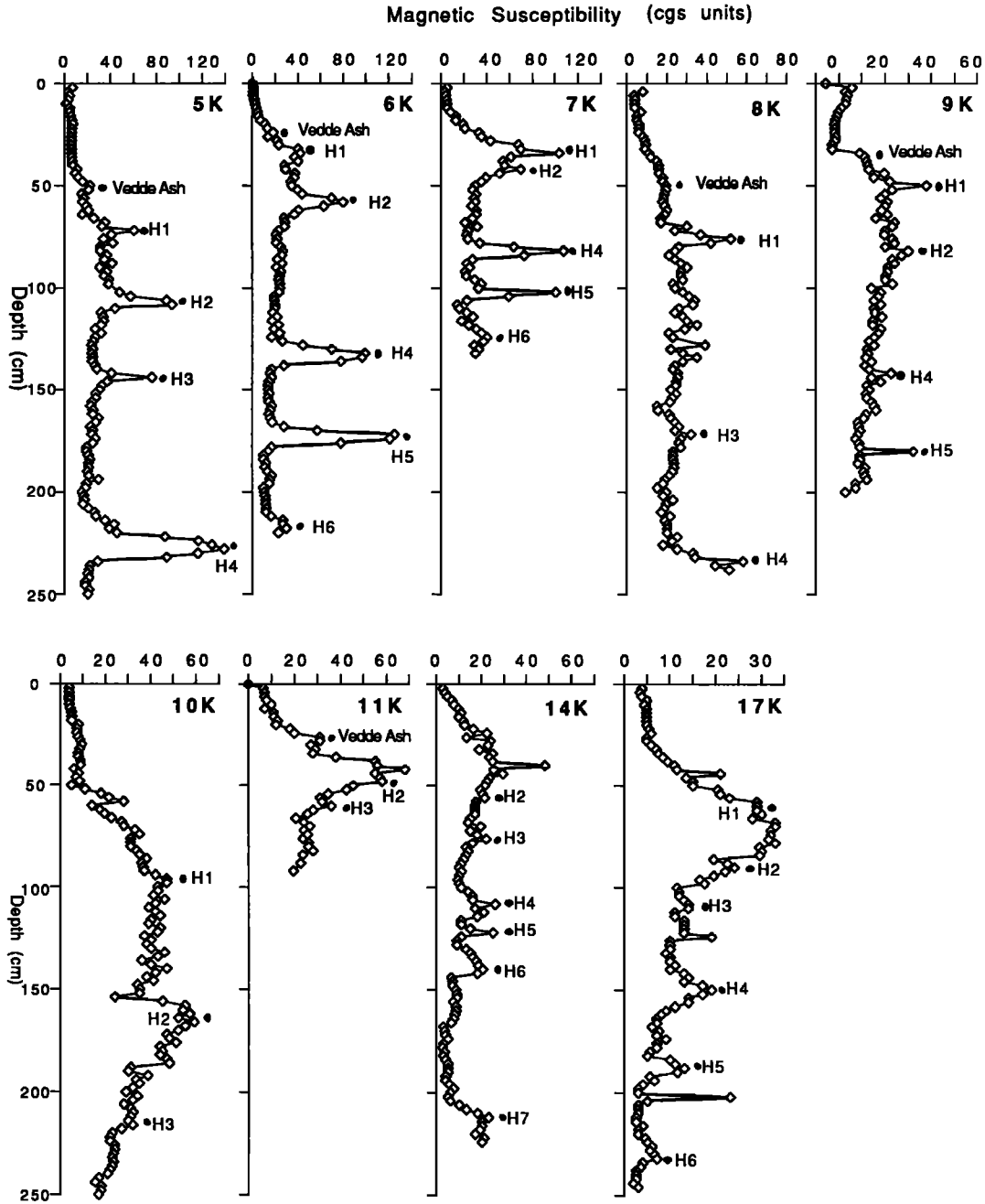


**Figure 9.** Bulk magnetic susceptibility with depth in the nine BOFS cores studied. The most prominent horizons for correlation are the peaks corresponding to Heinrich layers, which are marked H1-H7.

the X radiographs are often only 1 or 2 cm thick, and may be missed entirely by this sampling strategy.

### Carbonate Content

Carbonate (or inorganic carbon present in  $\text{CaCO}_3$ , expressed as  $C_i$ ) is predominantly a measure of the amount of biogenic carbonate from whole and fragmented foraminiferal tests and coccolith remains present in the sediment. Detrital carbonate also occurs as lithic fragments amongst the ice-rafted material deposited during Heinrich events. In general, the  $C_i$  profiles are characterized by low levels during the glacial (1-4%  $C_i$ ) and values increase rapidly around Termination 1A to high levels in the Holocene (8-10%  $C_i$ ) [Manighetti and McCave, this issue]. Carbonate content is a function not only of biogenic productivity, but also of dissolution and dilution by terrigenous material. Because there are so many influences upon it, this property may be difficult to correlate with confidence. Spatial variation in water temperature, ice cover, depth, and proximity to sources of terrigenous input will all affect the levels of carbonate in the cores. In addition, the architecture of the profiles is insufficiently distinctive over much of the record to provide more than a general guide to correlation in the short term. No points have been correlated solely on the basis of  $C_i$ , but similarities have been used as supporting evidence for correlations in other properties.

### Ash Correlation

For correlation purposes, the presence of ash peaks is often considered a means of establishing reliable chronological tie points across a suite of cores. In the northeast Atlantic, the Vedde Ash peak is usually assigned a  $^{14}\text{C}$  (atmospheric) age of 10,600 years [Mangerud et al., 1984]. This age has been recently revised to around 10,300 years [Bard et al., 1993b], which corresponds to a calibrated age of 12,152 years. However, as demonstrated earlier, the position of the peak of ash abundance will have been moved downward by homogenous bioturbation, perhaps by 8 cm or more, and will lie among foraminifera recording an older age, depending upon the sedimentation rate. Since the sedimentation rates in the BOFS cores vary from less than 2 to more than 10  $\text{cm ka}^{-1}$ , identification of the ash does not guarantee chronological correlation. In fact, the ash is most unlikely to be mixed to similar age levels in all cores. It may be more accurate to correct for differential sedimentation rate by assuming that homogenous bioturbation affects all cores to a similar depth, then assigning a  $^{14}\text{C}$  age of 10,300 (12,152 calendar years) to the interval 6-8 cm above the peak of ash abundance. This approach was adopted in the development of age models for the BOFS cores. The positions of the ash peaks are given in Table 3.

### Conclusions

The objective of this study has been to document the series of observations, measurements, calculations and assumptions involved in the construction of age models for the BOFS cores. We have constructed a calibrated AMS  $^{14}\text{C}$  model for core 5K based mainly on *G. bulloides* and *N. pachyderma* (s)

dates, which minimizes the effect of bioturbation of abundance gradients on age. A simple homogenous bioturbation model has been used with different mixing depths to assess the age offsets generated by such gradients. We find possible differences of 2.5-3 ka between the two species across Termination 1A, with mixing depths of 8-10 cm. *G. bulloides* ages are least biased during the Holocene, whereas *N. pachyderma* (s) dates are good below Termination 1A. The age of fine carbonate ( $<10 \mu\text{m}$ ) should show only minor offsets from "unbioturbated" ages, provided that the material is of primary biogenic and not detrital origin. The mixing depth for core 5K was assessed by examining dispersal of the Vedde Ash, and a value of roughly 8 cm was found to be characteristic of sand-sized material.

Extension of the core 5K model to other cores in the suite was achieved by correlation of landmarks in  $\delta^{18}\text{O}$ , magnetic susceptibility, X radiography,  $\delta^{13}\text{C}$ , and ash layers, assisted by carbonate-carbon and water content data. Heinrich zones were recognised and dated at 17,500, 25,150, 31,200, 43,100, 54,700, 69,700 and 130,000 (all consistently calendar years). Dating of these events is hampered by the strong abundance gradients associated with them, and the blocking effect they have upon bioturbation.

**Acknowledgements.** We thank David Page and Mike Hall for assistance with foram picking and isotopic analyses and Gillian Foreman for sedimentology. Perceptive discussions with Mark Hallworth and John Thomson were of great benefit in developing the ideas presented here, and we are grateful to J. Thomson and E. Bard for their reviews. This research was supported by NERC grant GST/02/436. BOFS publication # 197.

### References

- Andree, M., et al.,  $^{14}\text{C}$  measurements on foraminifera of deep sea core V28-238 and their preliminary interpretation, *Nucl. Instrum. Methods Phys. Res., Sect. B*, 5, 340-345, 1984.
- Bard, E., M. Arnold, J. Duprat, J. Moyes and J.-C. Duplessy, Reconstruction of the last deglaciation: Deconvolved records of  $\delta^{18}\text{O}$  profiles, micropaleontological variations and accelerator mass spectrometric  $^{14}\text{C}$  dating, *Clim. Dyn.*, 1, 101-112, 1987.
- Bard, E., M. Arnold, R. G. Fairbanks and B. Hamelin,  $^{230}\text{Th}$ - $^{234}\text{U}$  and  $^{14}\text{C}$  ages obtained by mass spectrometry on corals, *Radiocarbon*, 35, 191-199, 1993a.
- Bard, E., M. Arnold, J. Mangerud, M. Pateme, L. Labeyrie, J. Duprat, M. A. Melieres and E. Sonstegaard, Past gradients of the atmosphere-sea surface  $^{14}\text{C}$  gradient. Example of the North Atlantic during the Younger Dryas climatic event. *Terra Abstr.* 5, 14, paper presented at EUG VII Strasbourg, France, April 4-8, 1993b.
- Berger, W. H. and G. R. Heath Vertical mixing in pelagic sediments, *J. Mar. Res.*, 26: 134-143, 1968.
- Bond, G., et al., Evidence for massive discharges of icebergs into the North Atlantic ocean during the last glacial period, *Nature*, 360, 245-249, 1992.
- Bond, G., W. Broecker, S. Johnsen, J. McManus, L. Labeyrie and G. Bonani, Correlations between climate records from North Atlantic sediments and Greenland ice, *Nature*, 365, 143-147, 1993.
- Broecker, W., A. Mix, M. Andree and H. Oeschger, Radiocarbon measurements on coexisting benthic and planktic foraminifera shells: potential for reconstructing ocean ventilation times over the past 20,000 years., *Nucl. Instrum. Methods Phys., Sect. B*, 5, 331-339, 1984.

- Broecker, W. S., M. Andree, W. Wolfl, H. Oeschger, G. Bonani, J. Kennett and D. Peteet, The chronology of the last deglaciation: Implications to the cause of the Younger Dryas event. *Paleoceanography*, 3, 1-19, 1988.
- Broecker, W., G. Bond, M. Klas, E. Clark and J. McManus, Origin of the northern Atlantic's Heinrich events, *Clim. Dyn.*, 6, 265-273, 1992.
- Erez, J., Vital effect on stable isotopic composition seen in foraminifera and coral skeletons, *Nature*, 273, 199-202, 1978.
- Grousset, F. E., L. Labeyrie, J. A. Sinko, M. Cremer, G. Bond, J. Duprat, E. Cortijo and S. Huon, Patterns of ice rafted detritus in the glacial North Atlantic (40-45°N), *Paleoceanography*, 8, 175-192, 1993.
- Guinasso, N. L. and D. R. Schink, Quantitative estimates of biological mixing rates in abyssal sediments, *J. Geophys. Res.*, 80, 3032-3043, 1975.
- Heinrich, H., Origin and consequences of cyclic ice rafting in the northeast Atlantic Ocean during the past 130,000 years, *Quat. Res.*, 29, 143-152, 1988.
- Imbrie, J., J. D. Hays, D. G. Martinson, A. McIntyre, A. C. Mix, J. J. Morley, N. G. Pisias, W. L. Prell and N. J. Shackleton, The orbital theory of Pleistocene climate: Support from a revised chronology of the marine  $\delta^{18}\text{O}$  record, in *Milankovitch and Climate*, edited by A. L. Berger *et al.*, pp. 269-305, D. Reidel, Norwell, Mass., 1984.
- Jones, K. P. N., I. N. McCave and P. D. Patel, A computer-interfaced sedigraph for modal size analysis of fine-grained sediment, *Sedimentology*, 35, 163-172, 1988.
- Kipp, N., New transfer function for estimating past sea surface conditions from sea bed distribution of planktonic foraminiferal assemblages in the North Atlantic, *Geol. Soc. Am. Mem.*, 145, 3-41, 1976.
- Lunel, T., Trace metal concentrations and isotopes as tracers of oceanic processes, Ph.D. thesis, 169pp., Univ. of Cambridge, Cambridge, England, 1990.
- Mangerud, J., S. E. Lie, H. Fumees, I. L. Kristiansen and L. Lomo, A Younger Dryas ash bed in Western Norway, and its possible correlations with tephra in cores from the Norwegian Sea and the North Atlantic, *Quat. Res.*, 21, 85-104, 1984.
- Manighetti, B., The glacial to Holocene sedimentary regime in the northeast Atlantic Ocean, Ph.D. thesis, 218pp., Univ. of Cambridge, Cambridge, England, 1993.
- Manighetti, B. and I. N. McCave, Depositional fluxes, palaeoproductivity and ice rafting in the NE Atlantic over the past 30 ka. *Paleoceanography*, this issue.
- Maslin M.A., A study of the palaeoceanography of the NE Atlantic in the Late Pleistocene, Ph.D. thesis, 164 pp., Univ. of Cambridge, Cambridge, England, 1993.
- McCave, I. N., Leg 3, Benthic Studies, of the Biogeochemical Ocean Flux Study between 47°N and 60°N along 20°W in the northeast Atlantic Ocean, cruise report, Univ. of Cambridge, Cambridge, England, 1989.
- McCave, I. N., Biological pumping upwards of the coarse fraction of deep-sea sediments. *J. Sedimentol. Petrol.*, 58, 148-158, 1988.
- Nozaki, Y., J. K. Cochran, K. K. Turekian and G. Keller, Radiocarbon and  $^{210}\text{Pb}$  distribution in submersible-taken deep-sea cores from project FAMOUS, *Earth Planet. Sci. Lett.*, 34, 167-173, 1977.
- Paull, C. K., S. J. Hills, H. R. Thierstein, G. Bonani and W. Wolfl,  $^{14}\text{C}$  offsets and apparently non-synchronous  $\delta^{18}\text{O}$  stratigraphies between nannofossil and foraminiferal pelagic carbonates, *Quat. Res.*, 35, 274-290, 1991.
- Peng, T. -H. and W. S. Broecker, The impacts of bioturbation on the age difference between benthic and planktonic foraminifera in deep sea sediments., *Nucl. Instrum. Methods Phys. Res., Sect. B*, 5, 346-352, 1984.
- Peng, T. -H., W. S. Broecker, G. Kipphut and N. J. Shackleton, Benthic mixing in deep sea cores as determined by  $^{14}\text{C}$  dating and its implications regarding climate stratigraphy and the fate of fossil fuel  $\text{CO}_2$ , in *The Fate of Fossil Fuel  $\text{CO}_2$  in the ocean*, edited by N. Andersen and A. Malahoff, pp. 355-374, Plenum, New York, 1977.
- Ruddiman, W. F. and A. McIntyre, Northeast Atlantic paleoclimatic changes over the past 600,000 years, *Geol. Soc. Am. Mem.*, 145, 111-146, 1976.
- Ruddiman, W. and A. McIntyre, The North Atlantic ocean during the last deglaciation, *Palaeogeogr. Palaeoclimatol. Palaeoecol.*, 35, 145-214, 1981.
- Ruddiman, W. F., C. D. Sancetta and A. McIntyre, Glacial/Interglacial response rate of subpolar North Atlantic waters to climatic change: the record in oceanic sediments, *Philos. Trans. R. Soc. London, Ser. B*, 280, 119-142, 1977.
- Ruddiman, W. F., G. A. Jones, T. H. Peng, L. K. Glover, B. P. Glass and P. J. Liebertz, Tests for size and shape dependency in deep-sea mixing, *Sediment. Geol.*, 25, 257-276, 1980.
- Schiffelbein, P., Extracting the benthic mixing impulse response function: A constrained deconvolution technique, *Mar. Geol.*, 64, 313-336, 1985.
- Shackleton, N. J. and M. A. Hall, Stable isotope history of the Pleistocene at ODP site 677, *Proc. Ocean Drill. Program, Sci. Results*, 111, 295-316, 1989.
- Stuiver, M. and P. J. Reimer, Extended  $^{14}\text{C}$  data base and revised calib 3.0  $^{14}\text{C}$  age calibration program, *Radiocarbon*, 35, 215-230, 1993.
- Stuiver, M. and T. F. Braziunas, Modelling atmospheric  $^{14}\text{C}$  influences and  $^{14}\text{C}$  ages of marine samples back to 10,000 BC, *Radiocarbon*, 35, 137-189, 1993.
- Thomson, J., S. Colley, R. Anderson, G. T. Cook and A. B. MacKenzie,  $^{210}\text{Pb}$  in the sediments and water column of the Northeast Atlantic from 47-59°N along 20°W, *Earth Planet. Sci. Letts.*, 115, 75-87, 1993a.
- Thomson, J., S. Colley, R. Anderson, G. T. Cook, A. B. MacKenzie and D. D. Harkness, Holocene sediment fluxes in the Northeast Atlantic from  $^{230}\text{Th}_{\text{excess}}$  and radiocarbon measurements, *Paleoceanography*, 6, 631-650, 1993b.
- Wheatcroft, R. A., Experimental tests for particle size-dependent bioturbation in the deep ocean, *Limnol. Oceanogr.*, 37, 90-104, 1992.
- Zangger, E. and I. N. McCave, A redesigned kasten core barrel and sampling technique, *Mar. Geol.*, 94, 165-171, 1990.

B. Manighetti and I. N. McCave, Department of Earth Sciences, University of Cambridge, Downing Street, Cambridge, CB2 3EQ England.(e-mail B. Manighetti@esc. cam. ac. uk)

M. Maslin, Geologisch-Palaontologisches Institut, Universitat Kiel, Kiel, Germany.

N. J. Shackleton, Godwin Laboratory, University of Cambridge, Free School Lane, Cambridge, CB2 3RS, England.

(Received November 23, 1994; revised June 20, 1994; accepted November 16, 1994.)